Microstrip Varactor-Tuned Millimeter-Wave IMPATT Diode Oscillators

EDGAR J. DENLINGER, MEMBER, IEEE, JEROME ROSEN, MEMBER, IEEE, EDWARD MYKIETYN, AND EUGENE C. McDERMOTT, JR.

Abstract—**Varactor-tuned millimeter-wave IMPATT diode oscillators in microstrip form using chip-mounted diodes are described. A nearly level output power of 28 ± 8 mW was achieved over a 6-GHz tuning range. Tunable bandwidths as high as 8 GHz with 6–26 mW of power were obtained from a single source. P-type epitaxial silicon IMPATT diodes were used for both the active device and the tuning varactor functions.**

I. INTRODUCTION

TUNABLE millimeter-wave sources are becoming key devices in many types of systems. Where rapid tuning and reasonably high power are required, a varactor-tuned IMPATT diode source is an excellent candidate for such an application as a local oscillator for a wide-band millimeter-wave receiver. Alternative tuning mechanisms include YIG tuning [1], which is too slow for many applications and requires extremely high bias magnetic fields, and bias current tuning [2] which results in a large variation of output power over a wide frequency tuning range.

This paper describes a varactor-tuned millimeter-wave IMPATT diode oscillator built in microstrip form. Unpackaged devices are used to minimize parasitics in order to maximize the tuning bandwidth. P-type IMPATT diodes are utilized for the power source and also for the varactor tuning function. These complimentary P-type IMPATT diodes can be used more advantageously than conventional n-type IMPATTs because of their lower noise characteristics [3]. The tunable oscillator can be easily integrated with other receiver components into a small microwave integrated circuit (MIC) package.

II. TECHNICAL DISCUSSION

A. RF Power Source

The power source is a complementary N^+-P-P^+-type IMPATT diode which had been proven to offer high efficiency, high power, and low noise operation at *K*- and *Ka*-band frequencies in a waveguide disk-cavity structure [3]. This type of diode has a narrower effective avalanche zone compared with that of a conventional P^+-N-N^+ silicon structure with an identical carrier concentration profile in the depletion region because of the difference between electron and hole ionization coefficients. As a result, there is less fluctuation in the transit angle for the carriers in the complementary IMPATT, leading to an increase in negative resistance, a higher conversion efficiency, and a reduction in FM noise.

Because of the extreme importance of reducing the losses in a series-resonant circuit of a varactor-tuned oscillator, it was necessary to choose an IMPATT diode with the lowest possible contact resistance. For this reason a diode wafer with the characteristics shown in Table I was chosen. The average specific contact resistance of the diode was determined by using a standard *Q*-measurement technique with a UHF coaxial cavity [4]. The maximum power efficiency and mechanical tuning capability of these diodes have been reported earlier [3].

In our initial calculations we had assumed that the IMPATT capacitance of the oscillating diode is very nearly the same as that measured just before breakdown on a capacitance bridge. However, according to a recent paper by Ohtomo [5], the capacitance depends on bias current and frequency and can be more than a factor of 2 lower than the capacitance bridge measurement near breakdown. Because of the difficulty in making an impedance measurement at *Ka* band, Ohtomo's *X*-band impedance results were normalized to the diode's breakdown capacitance and avalanche frequency and then scaled up to *Ka* band. Such a scaled plot of the ratio of diode operating

TABLE I
IMPATT DIODE CHARACTERISTICS

Parameter	Value
1. Breakdown Capacitance	0.22 - 0.35 pF
2. Breakdown Voltage	31 - 35 v
3. Doping Density	2×10^{16} cm^{-3}
4. Average Specific Contact Resistance	4×10^{-6} $\Omega\text{-cm}^2$
5. Metallization	Chrome/Gold
6. P^+ Layer Dopant and Resistivity	Boron/0.001 Ω-cm
7. N^+ Layer Dopant and Resistivity	Phosphorous/0.0015 Ω-cm
8. Maximum Power/Efficiency in Waveguide	500 mW/10%
9. Mechanical Tuning Results	
a) Tuning Range	26.5-40 GHz
b) Minimum Power/Efficiency	360 mW/6.5%

Manuscript received April 14, 1975; revised August 18, 1975. This work was supported by the Naval Electronics Laboratory Center, San Diego, Calif., under Contract N00123-74-C-2027.

The authors are with the RCA Laboratories, David Sarnoff Research Center, Princeton, N.J. 08540.

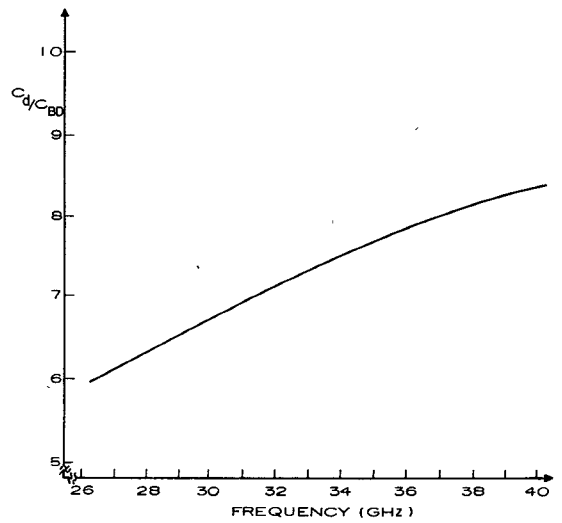

Fig. 1. Normalized IMPATT capacitance C_d/C_{BD} as a function of frequency.

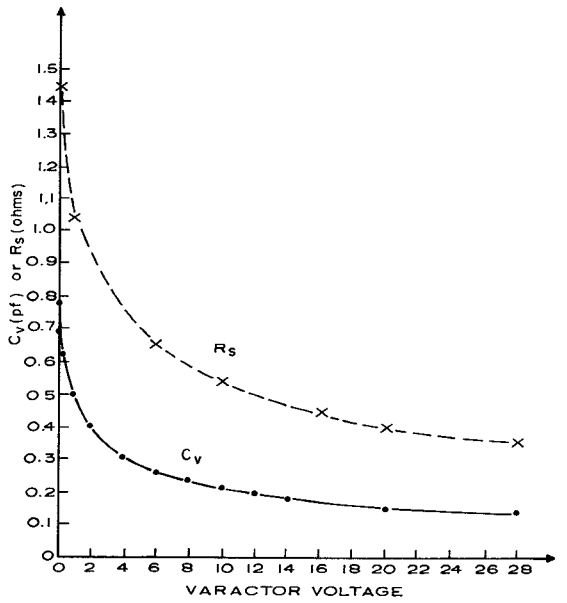

Fig. 2. Varactor series resistance and capacitance as a function of bias voltage.

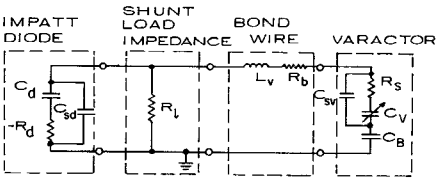

Fig. 3. Equivalent circuit of oscillator.

capacitance to breakdown capacitance as a function of frequency is shown in Fig. 1. The scaling was based on experimental results with IMPATT diodes oscillating with known inductances, a bias current in the 60–100 mA range, and an assumed avalanche frequency of 16 GHz. The values of capacitance obtained from Fig. 1 must be used in designing the resonant circuit for the tunable oscillator, as will be shown later.

B. Tuning Varactor

The important parameters for the varactor are the capacitance ratio $C_{\max}/C_{\min}$, the capacitance near breakdown $C_{\min}$, and the series resistance R_s. For a wide tunable bandwidth, the capacitance ratio should be large while $C_{\min}$ should be small compared to the IMPATT's effective capacitance. The series resistance R_s must be small enough so that the total resistance of the circuit external to the IMPATT diode does not exceed the available negative resistance. Fig. 2 shows experimental curves of R_s and C_v as a function of voltage for typical P-type IMPATT diodes which were used as varactors in the tunable oscillator experiments. These values were obtained from coaxial cavity resonator measurements at L band and correspond to a varactor cutoff frequency F_{co} of 3498 GHz near breakdown and 141 GHz at zero bias.

C. Oscillator Configuration

A commonly used type of varactor-tuned oscillator at lower frequencies is a series-tuned circuit, where the transformed load impedance is in series with the active device and the varactor. Cawsey's theoretical study [6] has shown that series tuning gives a wider tunable bandwidth than can be obtained with parallel tuning methods. Because of practical considerations, we chose Large's RF circuit [7] which uses a varactor in series with the active device, but the output power is taken directly in parallel with it. This circuit, shown in Fig. 3, provides a theoretical tuning bandwidth very close to that obtained with the series load as long as the load impedance is high ($R_l \geq$ 200 Ω). For oscillations to occur over the desired frequency range, the following requirements must be satisfied:

$$\text{Im } (Z_L) = \frac{1}{\omega(C_d + C_{sd})} \tag{1}$$

$$\text{Re } (Z_L) < |-R_d| \tag{2}$$

where Z_L is the impedance of the circuit external to the IMPATT diode, and C_d and R_d are, respectively, the capacitance and the equivalent negative series resistance of the IMPATT diode. Both the IMPATT and the varactor diodes have small stray shunt capacitances C_{sd} and C_{sv}, respectively, that are associated with the bond wire connections. The values of the capacitances are estimated to be less than 0.02 pF. Assuming an infinite impedance presented by the bias filters (and a total resistance $R_v = R_b + R_s$ in the varactor branch of the circuit including the resistances of the varactor and the bond wire), (1) becomes

$$\frac{1}{\omega(C_d + C_{sd})} = \frac{\left(\omega L_v - \dfrac{1}{\omega(C_v + C_{sv})}\right)}{\left(\dfrac{R_v + R_l}{R_l}\right)^2 + \left[\dfrac{\omega L_v - [1/\omega(C_v + C_{sv})]}{R_l}\right]^2}. \tag{3}$$

For large values of R_l,

$$\frac{1}{\omega(C_d + C_{sd})} \cong \omega L_v - \frac{1}{\omega(C_v + C_{sv})}. \quad (4)$$

The tuning bandwidth then is given by

$$\frac{F_2}{F_1} = \left(\frac{[1/(C_{v2} + C_{sv})] + [1/(C_{d2} + C_{sd})]}{[1/(C_{v1} + C_{sv})] + [1/(C_{d1} + C_{sd})]}\right)^{1/2}. \quad (5)$$

As was pointed out before, we must use the effective values of IMPATT capacitance which are frequency dependent. Thus C_{d1} and C_{d2} are the IMPATT capacitances at frequencies F_1 and F_2. The required inductance L_v for a given starting frequency F_1 is given by

$$L_v = \frac{1}{(2\pi F_1)^2}\left[\frac{1}{(C_{d1} + C_{sd})} + \frac{1}{(C_{v1} + C_{sv})}\right]. \quad (6)$$

Equation (2), in terms of the varactor and load circuit parameters, becomes

$$\frac{R_v + \dfrac{\{\omega L_v - [1/\omega(C_v + C_{sv})]\}^2}{(R_v + R_l)}}{1 + \dfrac{R_v}{R_l} + \dfrac{\{\omega L_v - [1/\omega(C_v + C_{sv})]\}^2}{R_l(R_v + R_l)}} < |R_d|. \quad (7)$$

To estimate the power output from the oscillator, the following equations can be used:

$$\frac{P_v}{P_l} = \frac{R_l}{R_v}\left\{1 + \left[\frac{\omega L_v - 1/\omega(C_v + C_{sv})}{R_v}\right]^2\right\}^{-1} \quad (8)$$

$$P_l = \frac{P_D}{1 + (P_v/P_l)} \quad (9)$$

where P_v and P_l are the amounts of power dissipated in the varactor and the load, respectively, while P_D is the power available from the IMPATT diode.

III. DESCRIPTION OF CIRCUIT COMPONENTS

Microstrip made of 0.010-in-thick Duroid was chosen as the transmission line for the oscillator because of its simplicity and ease of mounting diodes in shunt with the line. The line was enclosed in a rectangular channel of height 0.100 in and width 0.130 in. These dimensions were found from both theory [8] and experiment to be necessary in order to prevent waveguide modes from propagating.

For the microstrip–waveguide transition a cosine-tapered ridge waveguide transition was made similar to that developed by Saul [9]. As shown in Fig. 4, it consisted of a 1.4-in-long ridgeline transformer section with the ridge height varying as the cosine function over the interval 0 to π. The ridge height at one end is such as to leave a gap equal to the thickness of the microstrip line. An overlap of ~0.010 in between the microstrip line and the ridge was found to be optimum. With the shielded microstrip configuration, we did not require the cavitylike

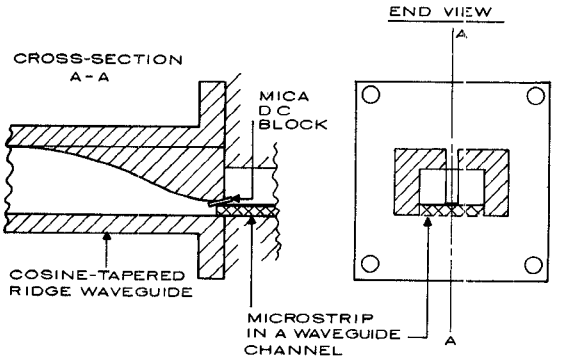

Fig. 4. Broad-band microstrip–waveguide transition.

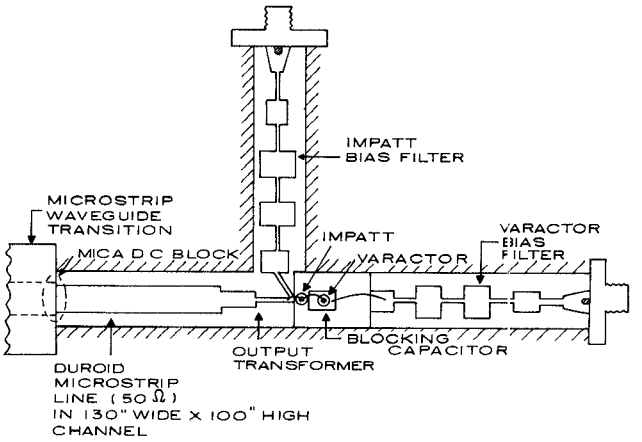

Fig. 5. Oscillator circuit.

structure used by Saul at the waveguide–microstrip interface since the enclosed microstrip did not show any radiation problems. The total loss of a 1-in-long 50-Ω microstrip line with a transition at each end was ~1 dB across the waveguide band. After insulating the line from the ridge of the transition with a 0.5-mil mica sheet, there was no discernible change in loss.

For achieving broad-band performance a nine-section Chebyshev band-reject filter was designed and utilized in both the IMPATT and varactor bias circuits, as shown in Fig. 5. The filter consisted of a cascade of transmission lines of electrically commensurate lengths but unequal impedances [10], [11]. The design passband-ripple VSWR and maximum rejection are 1.05:1 and 49.61 dB, respectively. The line length was specified so that maximum rejection could occur at 33 GHz, neglecting junction effects and dispersion. At 26.5 and 40 GHz the insertion loss is 45 and 44 dB, respectively. To evaluate the performance of the filter itself, a circuit was constructed in which the filter was coupled to 50-Ω microstrip lines with broad-band and microstrip–waveguide transitions at both ends. A swept frequency transmission loss measurement showed the rejection to decrease monotonically from 50 dB at 26.5 GHz to 33 dB at 40 GHz. Assuming the rejection characteristic to be shifted down in frequency due to improper line length, and recalculating the insertion loss based on maximum loss at 26.5 GHz, there is good agreement with the measured results. This would indicate a line length reduction of 25 percent to realize

the ideal response. However, since the rejection was greator than 30 dB this was not done.

For the tunable-oscillator circuit shown in Fig. 3 to have a bandwidth close to that of a simple series-resonant circuit, the load as seen at the IMPATT diode terminals must be large. A value of $R_l \geq 200\ \Omega$ was necessary to ensure that the resonant frequencies obtained from (3) and (4) are within 1 GHz of each other. This was accomplished by transforming from 50 to 300 Ω with either a single-section or two-section quarter-wave transformer. Very little difference in performance was seen with these two types of transformers.

The overall circuit configuration shown in Fig. 5 includes the bias filters, output transformer, and microstrip–waveguide transition that were discussed previously. Fig. 6 illustrates more clearly how the IMPATT and varactor diodes were mounted. The 10-pF blocking capacitor was an MOM (SiO_2) chip capacitor that was soldered to the bottom of the rectangular channel. Diodes were soldered into place while the inductor (L_v in Fig. 3) connecting them consisted of either a 1-mil-diam gold wire or a 1/2-mil-thick 2-mil-wide gold ribbon. This wire or ribbon was ultrasonically bonded to the diodes and to the output microstrip line. A second bond wire connected to the top of the blocking capacitor served as the first high-impedance section of the varactor bias filter. The equations used to determine the length of wire or ribbon to get the desired inductance between the IMPATT and varactor diodes are given as follows. For a wire of diameter d and length l (in inches) [12]

$$L_v(\text{nH}) = 5.08l\left[\ln\frac{4l}{d} - 1\right]. \tag{10}$$

For a ribbon of width w, thickness t, and length l (in inches)

$$L_v(\text{nH}) = 5.08l\left[\ln\frac{2l}{w+t} + 0.00249\right]. \tag{11}$$

A picture of the completed tunable oscillator structure is shown in Fig. 7.

IV. OSCILLATOR EXPERIMENTAL DATA

Various tunable oscillators were built for operation in the 24–40-GHz frequency range. The following paragraphs describe the power and frequency characteristics of some of these units.

An oscillator which had 6 GHz of tunable bandwidth and demonstrated a reasonably level output power of 28 ± 8 mW is shown in Fig. 8. The efficiency of this power source was about 1 percent. Note that the diodes were taken from the same wafer; however, the ones used for the varactor function were etched to a smaller size in order to get a large ratio between the breakdown capacitances of the IMPATT and varactor diodes, which is needed for achieving wide tunable bandwidths. The inductance of $L_v = 0.337$ nH connecting the two diodes was provided by a 22-mil-long 1-mil-diam gold bond wire looped in the air to minimize parasitics, as was shown in Fig. 6. Great

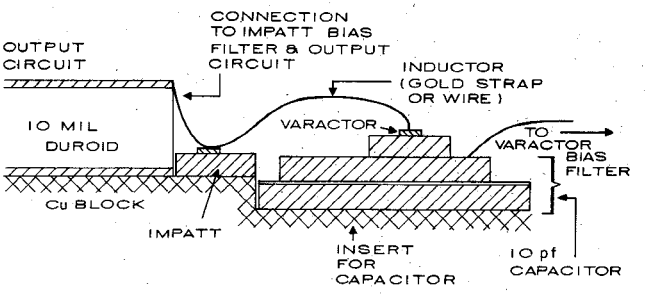

Fig. 6. Mounting configuration of diodes.

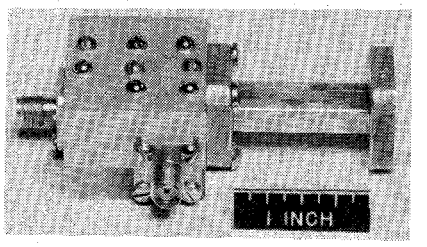

Fig. 7. Complete oscillator structure.

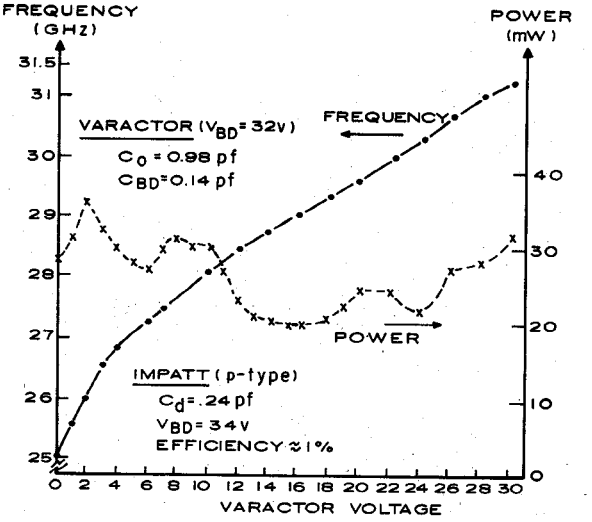

Fig. 8. Performance of oscillator with level output power.

care was taken to ensure that the varactor had very little leakage current in the reverse biased condition (typically less than 1 nA).

High output power from a tunable IMPATT source was demonstrated in the test shown in Fig. 9. However, a mode jump occurred at 32 GHz which was believed to be caused by an impedance loop in the output circuit [13] presented by the microstrip–waveguide transition. With the slightly larger difference between the IMPATT and varactor diode breakdown capacitance than was used in the previously described test, a theoretical tunable bandwidth of 7 GHz should have been achieved. Even though a mode jump did occur, the power levels of 40–150 mW and efficiencies of 1–3 percent indicate the feasibility of a high-power high-efficiency and wide tunable-bandwidth source in the *Ka*-band range.

Even greater tunability was achieved by increasing further the ratio of C_d to C_{v2} in the test with performance curves given in Fig. 10. A tunable bandwidth of 8 GHz with a power output of 6–26 mW was achieved before a

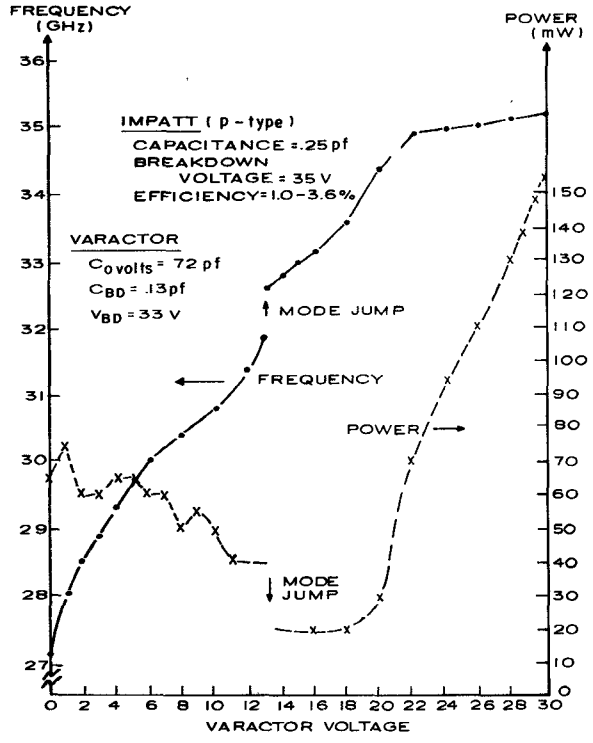

Fig. 9. Performance of oscillator with high output power.

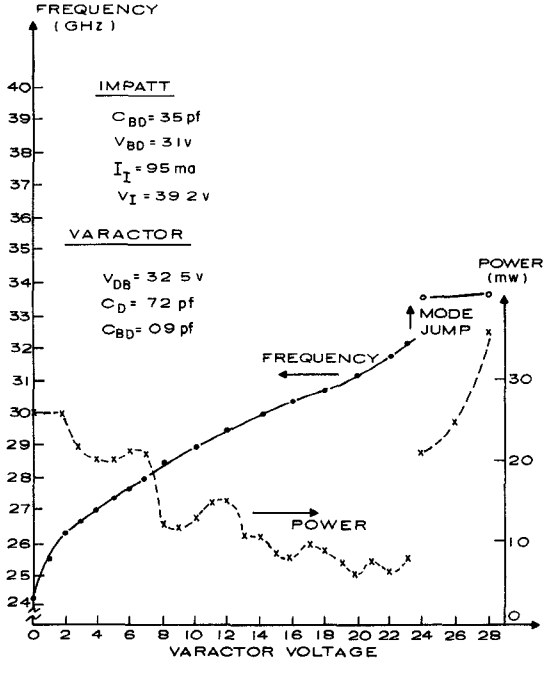

Fig. 10. Performance of oscillator with a large C_d/C_v ratio.

mode jump occurred above 32 GHz. Here the ratio of C_d to C_{v2} ($\simeq C_{BD}$ of varactor) is large enough to enable tuning from 24 to 35 GHz, a ratio $F2/F1$ of 1.47. This ratio is very close to that needed for covering the Ka-band range, namely $F2/F1 = 1.51$. If one extends the test tuning curve beyond the point where the mode jump occurs, it comes quite close to the theoretical upper limit of the tuning range at a varactor voltage of 30 V. In this test the inductor L_v consisted of a 23-mil-long 2-mil-wide ribbon connecting the diodes.

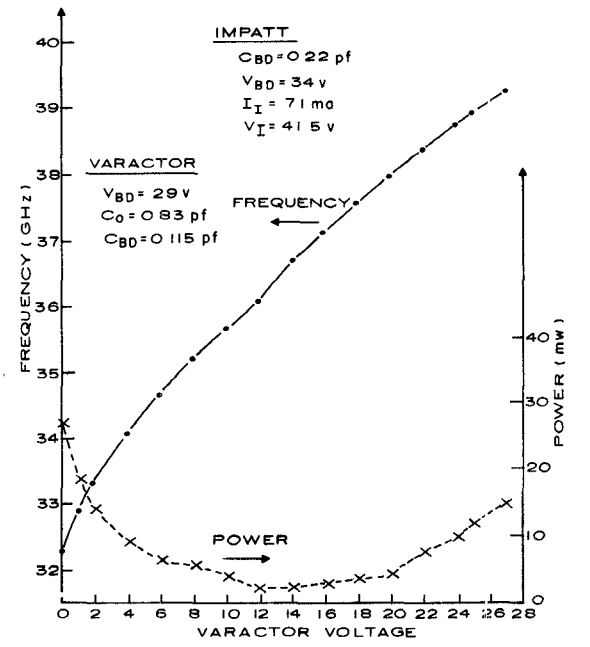

Fig. 11. Performance of oscillator operating in the upper half of the Ka-band range.

Another test which demonstrated the ability to tune over the upper half of the Ka-band range is shown in Fig. 11. In order to avoid a mode jump at the lower end of the tuning band, the length of the output quarter-wave transformer had to be shortened by 30 percent over that used in previous lower frequency tests. Also, further optimization of the circuit is needed to achieve a more level output-power characteristic.

A comparison of theoretical and experimental tuning bandwidths for the tests described previously is given in Table II. The IMPATT capacitances were determined from Fig. 1 and from the value of C_{BD} as measured on a capacitance bridge. The varactor capacitances C_{v1} and C_{v2} correspond to zero bias and breakdown capacitances, respectively. To obtain the inductance L_v, (6) is used with the frequency F_1 taken equal to the experimental value of F_1. Equations (10) and (11) have been used to calculate the inductance of the wire or ribbon connecting the two diodes, but the accuracy is only about ± 10 percent because of the difficulty in accurately measuring the wire or ribbon dimensions. As shown in the last two columns of the table, the agreement between theoretical and experimental values of F_2 is quite good. Most of the theoretical values were calculated with the stray shunt capacitances C_{sd} and C_{sv} taken equal to zero. However, for the case of Fig. 11, better agreement with experiment was obtained by assuming a finite value for C_{sv}. Overall, the simplified equations for tunable bandwidth given by (5) can be considered reasonably accurate.

V. CONCLUSIONS

We have succeeded in designing and building broad tunable-bandwidth millimeter-wave microstrip oscillators using P-type IMPATT diodes for both the power source and the tuning functions. Their reasonably level output power and compatibility with other components in a MIC pack-

TABLE II
COMPARISON OF THEORETICAL AND EXPERIMENTAL TUNING BANDWIDTHS

Figure	IMPATT Capacitance			Varactor Capacitance		L_v(nH)	F_2/F_1	F_1 exp.	F_2	
	C_{BD} (pF)	C_{d1} (pF)	C_{d2} (pF)	C_{v1} (pF)	C_{v2} (pF)				Theor.	Exper. *(Projected to V_{BD})
8.	0.24	0.137	0.168	0.98	0.14	0.337	1.25	25	31.4	31.1
9.	0.25	0.153	0.203	0.72	0.13	0.275	1.26	27	34	35*
10.	0.35	0.182	0.266	0.72	0.09	0.387	1.47	24	35.3	34.5*
11.	0.22	0.156	0.183	0.83	0.115	0.186	1.36	32.2	43.9	39.2
C_{sv}=0.02				0.85	0.135		1.30		41.9	

age make them ideal for use in wide-band millimeter-wave receivers. The low noise characteristic of the P-type IMPATT diodes is also extremely advantageous. We believe that with more effort, a single varactor-tuned IMPATT source could produce a fairly level output-power tuning characteristic over the full *Ka*-band range.

ACKNOWLEDGMENT

The authors wish to thank Dr. Y. S. Chiang and Dr. G. A. Swartz for their technical assistance.

REFERENCES

[1] R. E. Oyafuso and R. E. Brown, "Think young with agile YIG and varactor tuning," *Microwaves*, pp. 40–43, Dec. 1972.
[2] H. Kuno, "Current-tuned millimeter wave IMPATT diodes," presented at the 1974 Millimeter-Wave Techniques Conf., San Diego, Calif.
[3] G. A. Swartz, Y.-S. Chiang, C. P. Wen, and A. Gonzalez, "Performance of P-type epitaxial silicon millimeter-wave IMPATT diodes," *IEEE Trans. Electron Devices*, vol. ED-21, pp. 165–171, Feb. 1974.
[4] E. L. Ginzton, *Microwave Measurements*. New York: McGraw-Hill, 1957, ch. 9.
[5] M. Ohtomo, "Broad-band small-signal impedance characterization of silicon (Si) P^+-N-N^+ IMPATT diodes," *IEEE Trans. Microwave Theory Tech.*, vol. MTT-22, pp. 709–718, July 1974.
[6] D. Cawsey, "Wide-range tuning of solid-state microwave oscillators," *IEEE J. Solid State Circuits* (Corresp.), vol. SC-5 pp. 82–84, Apr. 1970.
[7] D. Large, "Octave band varactor-tuned diode sources," *Microwave J.*, vol. 13, pp. 49–51, Oct. 1970.
[8] M. V. Schneider, "Millimeter-wave integrated circuits," in *1973 G-MTT Symp. Dig.*, pp. 16–18.
[9] D. Saul, "Wideband microstrip components and the IFM discriminator," in *Proc. 1974 Millimeter-Wave Techniques Conf.*, vol. 2, pp. D4-1–D4-12.
[10] H. Seidel, "Synthesis of a class of microwave filters," *IRE Trans. Microwave Theory Tech.*, vol. MTT-5, pp. 107–114, Apr. 1957.
[11] R. Levy, "Tables of element values for the distributed low-pass prototype filter," *IEEE Trans. Microwave Theroy Tech. (Special Issue on Microwave Filters)*, vol. MTT-13, pp. 514–536, Sept. 1965.
[12] F. Grover, *Inductance Calculations: Working Formulas and Tables*. New York: Dover, 1946, ch. 5.
[13] C. Chao and G. I. Haddad, "Nonlinear behavior and bias modulation of an IMPATT diode oscillator," *IEEE Trans. Microwave Theory Tech.*, vol. MTT-21, pp. 619–630, Oct. 1973.